ac susceptibility of a $DyFe_{11}Ti$ single crystal

M. D. Kuz'min, L. M. García, M. Artigas, and J. Bartolomé
Instituto de Ciencia de Materiales de Aragón, Consejo Superior de Investigaciones Científicas, Universidad de Zaragoza, Plaza San Francisco S/N, 50009 Zaragoza, Spain

(Received 4 January 1996; revised manuscript received 1 April 1996)

A study of the ac initial magnetic susceptibility of a roughly spherical single crystal of $DyFe_{11}Ti$ is reported. Both the real and imaginary parts of the complex susceptibility have been measured in absolute units along the principal crystallographic directions, the results being practically identical for [100] and [110]. The underlying mechanisms—coherent magnetization rotation and domain-wall motion—are considered. It is demonstrated that the thermally activated domain-wall displacements provide the clue to understanding the main features of the temperature dependence of both the real and imaginary parts of the observed susceptibility. [S0163-1829(96)06026-2]

I. INTRODUCTION

Alternating-current susceptometry is a simple and useful tool widely employed to study magnetic systems. Its application to hard magnetic materials, however, has been so far limited to observation of anomalies associated with phase transitions. Such restricted practice is explained by the fact that ac susceptibility (which is in essence initial susceptibility) is an extrinsic property and as such it depends strongly on sample shape, microstructure, impurities, etc. While a good general understanding of intrinsic properties of intermetallic hard magnets has been achieved, their extrinsic properties, such as parameters of the domain structure and ac susceptibility remain far from being well studied. Experimental data are scarce and theoretical models are uncoordinated and inconclusive.

When measured on a polycrystalline sample, ac susceptibility has its characteristic anomalies smeared out considerably and new anomalies can appear due to impurities, such as interstitial hydrogen, which are sometimes mistaken for phase transitions (a collection of such misinterpretations is given in Refs. 1–3).

In order to enable its systematic quantitative analysis, ac susceptibility should be studied on single crystals shaped in some standard way, e.g., as spheres. Both real and imaginary parts of the susceptibility should be measured and the units should not be arbitrary. An attempt to accept this challenge has been recently undertaken by Chen, Skumryev, and Kronmüller[4] who studied the ac susceptibility of a monocrystalline $Nd_2Fe_{14}B$ sphere. Unfortunately, no satisfactory agreement was achieved between their theoretical model and experimental data. A definite merit of Ref. 4 is the clear demonstration of irrelevance of eddy current effects to ac susceptibility of hard magnetic materials at frequencies below 1 kHz by direct *ab initio* evaluation of the corresponding contribution to the ac susceptibility.

This work is a further attempt of a quantitative study of the ac susceptibility of hard magnetic materials. Our choice fell on $DyFe_{11}Ti$, an intermetallic compound whose anisotropic magnetic properties had been studied in great detail[5–9] and of which suitable single crystals were available.

$DyFe_{11}Ti$ is a ferrimagnet [T_C=534 K (Ref. 5)] with the $ThMn_{12}$ tetragonal structure, space group $I4/mmm$ (substitution of Ti is necessary to stabilize the structure as pure $DyFe_{12}$ does not exist). The anisotropy energy can thus be written as

$$F_a = K_1 \sin^2\theta + (K_2 + K_2' \cos 4\varphi)\sin^4\theta + (K_3 + K_3' \cos 4\varphi)\sin^6\theta, \quad (1)$$

where the spherical angles θ and φ describe orientation of the magnetization vector with respect to the crystallographic axes; K_1, K_2, etc. are the anisotropy constants. The easy direction at high temperatures coincides with the fourfold axis, or [001]; at lower temperatures it reorientates towards the basal plane remaining within the (110) or (110) planes, so that the angle φ is equal to $\pi/4 + n\pi/2$, where n=1,2,3,4 corresponds to four possible domains. Therefore, for some applications Eq. (1) can be simplified as follows:

$$F_a = K_1 \sin^2\theta + \overline{K_2}\sin^4\theta + \overline{K_3}\sin^6\theta, \quad (2)$$

$$\overline{K_2} = K_2 - K_2', \quad \overline{K_3} = K_3 - K_3'. \quad (3)$$

The nature of the spin reorientation transitions (SRT) in $DyFe_{11}Ti$ has been established not without some controversy. It was found that a continuous deviation of the easy axis from the [001] direction starts at $T_2 \approx 200$ K (Ref. 6) or $T_2 \approx 220$ K,[7] which constitutes a second-order spin reorientation transition (a more refined approach—extrapolation of the θ^2 vs T plot—yields T_2=191 K, see Fig. 1 of Ref. 10). The second transition occurs, according to Ref. 6, at T_1=58 K and is of the first order, meaning that the angle θ between the easy axis and [001] undergoes a discontinuous change from ~40° to 90° (in Ref. 6 the easy direction at low temperatures was identified as [100] rather than [110], the mistake was rectified later, see endnote 4 of Ref. 8).

A quite different view on the second transition was suggested in Ref. 7: at $T_1 \sim 120$ K a change of slope in the $\theta(T)$ dependence takes place (which was considered a second-order phase transition) however θ never reaches 90°, the maximum value being 80°. Upon a thorough study of the angular dependence of magnetization[9] the interpretation of this SRT given in Ref. 7 has been refuted. The phase transi-

tion has been confirmed to be of the first order; the two phases, with $\theta=40°$ and 90°, are essentially different and correspond to two different minima in the anisotropy energy; no minima have been found at intermediate values of θ. The apparently continuous variation of θ at $T\sim 50$–70 K is explained by coexistence of the 40° and 90° phases in that temperature interval, stabilized, in all likelihood, by magnetostatic energy.[9] Theoretically, the necessary conditions for the spontaneous spin reorientation transitions taking place in $DyFe_{11}Ti$ are the following: (1) $K_{\rm eff}=K_1+K_2+K_3=0$ at $T=T_1$; (2) $K_1=0$ at $T=T_2$.

In this work we shall concentrate primarily on the general evolution of the ac susceptibility of $DyFe_{11}Ti$ with temperature, including anomalies in the vicinity of T_2, believed to be characteristic of many hard magnetic materials. In contrast, the anomalies around T_1, peculiar to $DyFe_{11}Ti$, will receive less attention.

II. EXPERIMENT

The $DyFe_{11}Ti$ single crystal was prepared by Song-Quen Ji at Natuurkundig Laboratorium in Amsterdam using the Czochralski method in a tri-arc furnace. A piece cut from the original boule was polished with abrasive paper to make a rough sphere about 1.5 mm in diameter. The sphere was embedded into epoxy resin to form a solid block. That block was subsequently faceted with a diamond saw to obtain a prism whose base was perpendicular to the [001] crystal axis; that base was shaped as an isosceles rectangular triangle with the cathetuses along [100] and [010] and the hypotenuse along [110]. The prism could be easily glued with vacuum grease onto the sample holder, which had a plane parallel to the exciting field of the susceptometer.

The measurements were performed with an ac susceptometer under zero external dc field, described elsewhere.[11] The complex initial susceptibility, $\chi=\chi'-i\chi''$, was measured, where χ' is the component in phase with the exciting ac field and χ'' is the quadrature component. The exciting field had the amplitude of 1 Oe and the frequency of $\nu=120$ Hz. Before the measurements the sample was demagnetized by cooling it from room temperature down to 4.2 K. In this way the sample undergoes the transition to the low-temperature phase and divides itself into four types of domains with domain magnetization along [110], [110], [110], and [110]. It had been proved[9] that the magnetization at 4.2 K becomes zero after such a zero-field-cooling process. This was found to be a simple, efficient and cheap way of starting the measurements always from the same condition of full demagnetization. After this process the temperature was increased in steps and each point was measured upon waiting for the temperature to become stable within 0.1 K. To obtain absolute measurements, the susceptometer was calibrated against Mn Tutton salt. Dimensionless susceptibility was expressed in Gaussian units, the demagnetizing factor was taken equal to $N=4\pi/3\approx 4.19$.

The results of measurements along [100] and [110] are shown in Fig. 1. A rounded anomaly is observed in the real component (full symbols) and in the imaginary component (open symbols) at the first-order transition at T_1. At the second-order transition at T_2 a sharp peak is observed in the real component while just a low and rounded maximum appears in the imaginary component. Both directions, [100] and [110], give practically the same results, so they will be referred to as $\chi_\perp$, or $\chi'_\perp$ and $\chi''_\perp$, for the respective real and imaginary components.

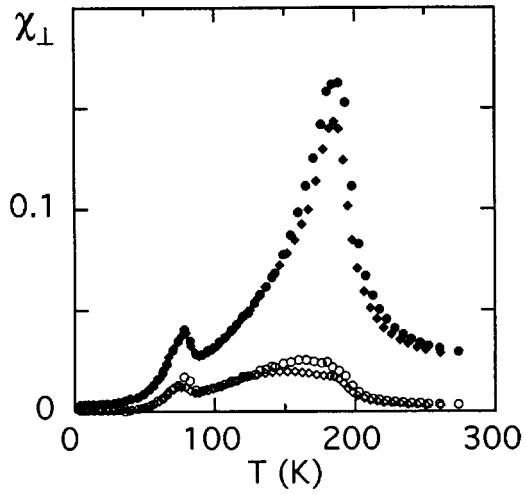

FIG. 1. Temperature dependence of transverse external ac susceptibility: (●) [100], real component, (○) [100], imaginary component; (◆) [110], real component; (◇) [110], imaginary component.

In Fig. 2 we depict the results along [001] which we denote as $\chi'_\parallel$ and $\chi''_\parallel$ for the real and imaginary components, respectively. $\chi'_\parallel$ increases continuously with temperature while $\chi''_\parallel$ shows a maximum at 200 K. Both curves show in common a small bump at T_1 and a sudden dip at T_2.

Frequency dependences of $\chi_\perp$ and $\chi_\parallel$, from 77 K to room temperature, have been measured in the range of 1 Hz to 1 kHz with a superconducting quantum interference device magnetometer using its ac susceptibility option (see Fig. 3). They show that the maximum in $\chi'_\perp$ and the dip in $\chi'_\parallel$ do not shift in temperature. Only the amplitude of the susceptibility shows a dependence on exciting frequency.

We observed directly the surface magnetic domain structure of a different single crystal. The shape of the crystal was an oblong ellipsoid, which main axes were 8, 2.3, and 0.5 mm polished from a platelet cut with its surface parallel to the (110) plane. The Bitter technique was employed, with a

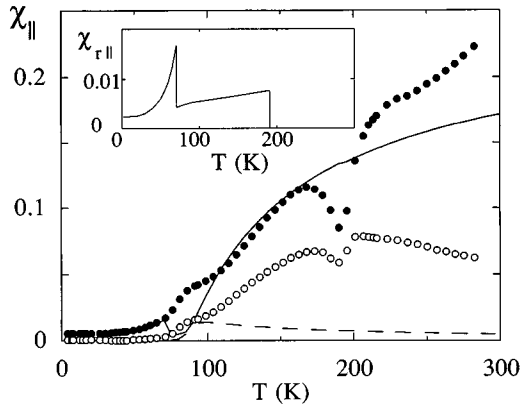

FIG. 2. Temperature dependence of external ac susceptibility along the [001] direction: (●) real component, experiment; (○) imaginary component, experiment; (–) real component, calculation; (---) imaginary component, calculation. Inset: Calculated contribution due to coherent spin rotations.

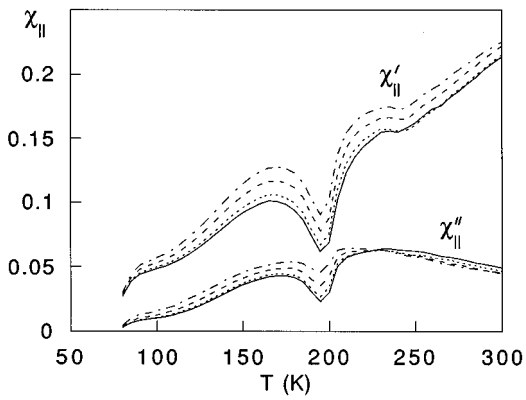

FIG. 3. Temperature dependence of external ac susceptibility along the [001] direction at various frequencies: (–) $\upsilon = 976$ Hz, (···) $\upsilon = 120$ Hz, (---) $\upsilon = 10$ Hz, (·-·-) $\upsilon = 1$ Hz.

visualizing ferrofluid of 0.03 mm particle size, and the observation was made with a metallographic microscope (amplification factor 250). The (110) sample surface was polished and the photo was taken in the center of the ellipsoid (Fig. 4). The sample had been previously demagnetized by cooling down to 4.2 K, as described earlier.

III. DATA ANALYSIS

A. Preliminaries

Examination of Figs. 1 and 2 reveals the presence of nonzero imaginary susceptibility. This fact, although described in previous works,[4,12] has not received sufficient attention so far. Let us denote the internal susceptibility as $\kappa \equiv \kappa' - i\kappa''$. Then the external susceptibility, $\chi \equiv \chi' - i\chi''$ can be found from the expression

$$\chi^{-1} = \kappa^{-1} + N, \tag{4}$$

or, separating the real and imaginary parts,

$$\chi' = \frac{\kappa' + N[(\kappa')^2 + (\kappa'')^2]}{(1 + N\kappa')^2 + (N\kappa'')^2}, \tag{5}$$

$$\chi'' = \frac{\kappa''}{(1 + N\kappa')^2 + (N\kappa'')^2}. \tag{6}$$

These expressions are well-known in ac susceptometry,[13,14] however their implications for hard magnetic materials have not been understood so far. The inverse transformation,

$$\kappa' = \frac{\chi' - N[(\chi')^2 + (\chi'')^2]}{(1 - N\chi')^2 + (N\chi'')^2}, \tag{7}$$

$$\kappa'' = \frac{\chi''}{(1 - N\chi')^2 + (N\chi'')^2}, \tag{8}$$

is obtained simply by permutation $\kappa \leftrightarrow \chi$, $N \leftrightarrow -N$.

Inspection of Eqs. (7) and (8) shows that when $\chi'' \ll \chi' \approx 1/N$ small errors in χ', χ'' or N may lead to large uncertainties in the corresponding values of κ' and κ'' (cf. Ref. 14). Such situation seems to take place near room temperature for $\chi_\parallel$ and at $T \approx T_2$ for $\chi_\perp$. The absolute values of the corresponding internal susceptibilities at the above temperatures should be therefore taken with caution. For this reason, we prefer to transform, by means of Eqs. (5) and (6), the theoretically found κ's into χ's and compare the latter directly with experimental data, rather than to ''correct the data for demagnetization.''

The two main sources of magnetic susceptibility in ferro- and ferrimagnets are coherent rotation of the magnetization vector and domain-wall motion (DWM). The coherent rotation process consists in spatially homogeneous tilting of all magnetic moments within a particular domain towards the ac exciting field. DWM is a process of inhomogeneous rotation of magnetic moments within the wall; in such a process the wall is effectively displaced and one of the two domains involved gains volume.

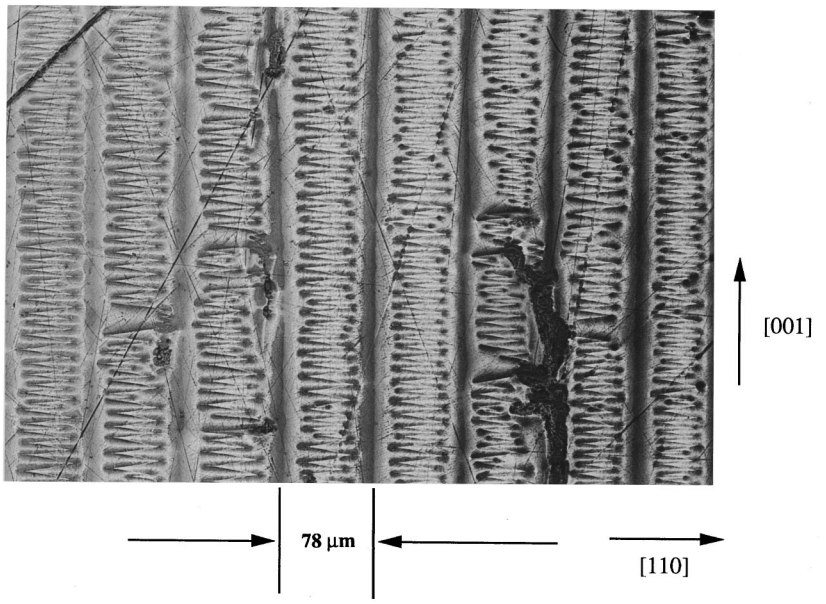

FIG. 4. Microscopic photograph of the stripe-type pattern of 180° domain walls, parallel to the c axis. The pattern was obtained with the Bitter technique on the surface of a $DyFe_{11}Ti$ single crystal at room temperature.

B. ac susceptibility due to coherent rotation of magnetization

Rotational susceptibility κ_r at low frequencies is expected to be purely real and fully determined by the bulk anisotropy constants. So its evaluation proceeds in two steps, first the bulk anisotropy constants are calculated as described in Appendix A starting from the crystal-field (CF) parameters and exchange constants of Ref. 6, and then κ_r is calculated following the straightforward but cumbersome procedure described in Appendix B.

In the temperature range above T_2 $\kappa_{r\parallel}=0$ and $\kappa_{r\perp}$ is given by Eq. (B2). Below T_2, where the azimuthal angle φ can take four different values $\varphi=\pi/4+n\pi/2$, with $n=1$, 2, 3 and 4, it is necessary to assume a particular distribution of domains to perform the calculation. In view of the near equivalence of the experimental results for [100] and [110], as seen in Fig. 1, we assume an equiprobable distribution of the $n=1$, 2, 3 and 4 domains. Thus, the theoretical expressions used in the calculations are Eq. (B10) for $\kappa_{r\parallel}$ and (B17) for $\kappa_{r\perp}$.

C. ac susceptibility due to DWM

Rotational susceptibility is usually small in comparison with a larger contribution from domain-wall motion, unless the latter vanishes for some reason. We shall now concentrate on DWM susceptibility, κ_d. Presence of domain walls separating domains with different values of magnetization along the direction of the ac field is evidently a necessary condition for a nonzero DWM susceptibility.

At room temperature classical stripe 180 ° domains are observed in $DyFe_{11}Ti$ (Fig. 4), the average domain width d being equal to 78 μm.[15] Similar domain structure has been detected in other easy-axis intermetallic hard magnets.[16–18] One can therefore assume with reason that this structure is stable in $DyFe_{11}Ti$ at temperatures down to T_2. As no experimental information on the domain structure in $DyFe_{11}Ti$ below T_2 is available at present, we shall consider some plausible hypotheses.

The canting of the magnetization that occurs at T_2 breaks the fourfold symmetry in the (001) plane, so the 180 ° walls transform into 180 °-2θ walls with simultaneous appearance of new types of walls separating domains with equal θ and different φ. The former type of domain walls (different θ, equal φ) contributes solely to $\chi_\parallel$, whereas the latter (equal θ, different φ) only contributes to $\chi_\perp$. Indeed, in recent NMR experiments two types of domain walls have been detected in the easy-cone phase of $Nd_2Co_{14}B$.[19]

On the basis of these considerations we understand that below T_1, when $\mathbf{M}_s\perp[001]$, DWM gives no contribution to $\kappa_\parallel$. Similarly, above T_2, when $\mathbf{M}_s\parallel[001]$, it does not contribute to $\kappa_\perp$. In these cases the intrinsic susceptibility is determined exclusively by the coherent magnetization rotation.

An elaborate particular case, which is believed to apply to permanent magnet materials, is that of narrow domain walls. In that case the potential hindering the DWM is approximately sinusoidal[20] with the amplitude proportional to[21] $\exp(-\pi\delta/\Lambda)$, and hence significant only when the wall thickness δ is not much larger than the lattice period in the direction perpendicular to the wall, Λ. For $DyFe_{11}Ti$ at $T>T_2$, a simple 180 ° domain structure is expected with the walls lying in the (110) planes; hence $\Lambda=a/\sqrt{2}\approx 6$ Å.

To estimate the wall thickness, one needs to know the value of the exchange stiffness, A, which can be deduced from inelastic neutron-scattering data. Since no such data for $DyFe_{11}Ti$ are available in literature, we shall evaluate A for $Nd_2Fe_{14}B$. The experimental dispersion curve[22] is parabolic at small wave numbers, $\epsilon=\epsilon_0+Dq^2$, with $D=2.5\times10^{-29}$ erg cm^2. Then, the exchange stiffness is given by[23] $A=(1/2)D(S/\Omega)=1.0\times10^{-6}$ erg/cm, where $S/\Omega=7.8\times10^{22}$ cm^{-3} is the *spin density*. Application of this value of A to $DyFe_{11}Ti$ is justified by the fact that the Curie points of $Nd_2Fe_{14}B$ and $DyFe_{11}Ti$ are close (588 and 534 K, respectively[24]) and the exchange stiffness of iron-rich magnets appears to be proportional to the T_C, cf. for pure iron ($T_C=1043$ K) $A=2.0\times10^{-6}$ erg/cm.[25]

The effective anisotropy constant at $T=200$ K is $K_{\rm eff}=K_1+K_2+K_3=5\times10^6$ erg/cm^3 (see Appendix A for details) and finally the wall thickness is $\delta=\pi(A/K_{\rm eff})^{1/2}=140$ Å. Thus, the amplitude of the intrinsic sinusoidal potential contains a small factor $e^{-73}\sim10^{-32}$ and this contribution to the hindering barrier can be neglected (this also justifies the application of the standard continuum formalism). Consequently, it seems reasonable to assume that the potential is caused mainly by defects. These are supposed to be small, sparsely distributed objects, so that the overall picture corresponds to the case of ''strong pinning'' as defined by Gaunt.[26]

The excitation by an alternating field produces two effects: the walls oscillate within the potential well created by the defect, or hop from well to well. The type of behavior depends on amplitude and frequency of the ac field. In the first case there is no imaginary component since there is no time delay in such reversible motion. On the contrary, the hopping process gives rise to both real and imaginary components, as occurs in the present case. Since two different types of domain walls are responsible for $\kappa_\parallel$ and $\kappa_\perp$, one may expect the hindering barriers to be different for the two directions. For simplicity hereafter we omit the subscripts $\parallel$ and $\perp$.

In the simplest approach we propose that the DW hopping process is thermally activated and may be ascribed a relaxation time τ obeying the Arrhenius law

$$\tau=\tau_0\exp(E/kT), \tag{9}$$

where E stands for the activation energy and $\tau_0\sim10^{-12}$ s is the characteristic time constant of ferromagnetic resonance. If just one type of defect existed, the susceptibility would be expressed by the Debye formula

$$\kappa_d=\frac{\kappa_0}{1+i\omega\tau}, \tag{10}$$

where κ_0 is the susceptibility in the static ($\omega\tau\ll1$) limit. κ_0 may depend on temperature and be related to various possible mechanisms, such as bulging of walls pinned at defects, considered by Kersten,[27] but we shall refrain from complicating the model and assume that κ_0 remains temperature independent.

The above expression holds for just one activation energy, however, a very broad distribution of energy barriers should be involved in the pinning of walls by defects, so averaging over the barrier distribution expressed as a function of acti-

vation energies $f(E)$ needs to be performed. The simplest distribution one may propose is rectangular, with barriers spanning from a minimum threshold value E_0 to a maximum E_0+W. The distribution height is W^{-1} to normalize to unity the integral of $f(E)$ over all energies.

The averaged real and imaginary susceptibilities are

$$\kappa_d'=\frac{\kappa_0}{W}\int_{E_0}^{E_0+W}\frac{dE}{1+(\omega\tau)^2}$$

and (11)

$$\kappa_d''=\frac{\kappa_0}{W}\int_{E_0}^{E_0+W}\frac{\omega\tau dE}{1+(\omega\tau)^2}.$$

It follows from Eq. (9) that $dE=kTd\tau/\tau$; applying this substitution to Eqs. (11) and integrating, one obtains the final expressions:

$$\kappa_d'=\frac{1}{2}\,kT\,\frac{\kappa_0}{W}\ln\left\{1+\left[\omega\tau_0\,\exp\left(\frac{E_0}{kT}\right)\right]^{-2}\right\} \tag{12}$$

and

$$\kappa_d''=kT\,\frac{\kappa_0}{W}\left\{\frac{\pi}{2}-\arctan\left[\omega\tau_0\,\exp\left(\frac{E_0}{kT}\right)\right]\right\}, \tag{13}$$

where $\omega=2\pi\nu$ is the measuring frequency and τ_0 is taken equal to 1×10^{-12} s.

D. Discussion

The calculation of the different components of the complex susceptibility comprised several steps. First, the rotational contribution was calculated starting from the crystal field and exchange parameters known for this compound from other sources (see Appendixes A and B). At each temperature the anisotropy constants were calculated following the procedure described in Appendix A and were subsequently substituted into either Eqs. (B1) and (B2), for $T>T_2$, or, for $T<T_2$, into Eqs. (B7) and (B8) in conjunction with Eqs. (B10) and (B17). The resulting κ_r (purely real) was then transformed into external susceptibility χ' using Eq. (5). At this stage χ'' was zero.

In Fig. 5 the resulting curve for $\chi_\perp'$ is drawn as a continuous line for $T>T_2$ and a dotted line for $T<T_2$. The fit is excellent for $T>T_2$, proving that only coherent rotation of the magnetic moments is responsible for $\chi_\perp'$ when $T>T_2$. Indeed, DWM gives no contribution since the spontaneous magnetization is perpendicular to the exciting field. The divergence of $\kappa_\perp'$ at $T=T_2$ results in the finite theoretical value of $1/N=3/4\pi\approx0.24$ for $\chi_\perp'$, which is somewhat higher than the experimental result.

However, below T_2 the coherent rotation contribution (dotted line) is much lower than the experimental $\chi_\perp'$; i.e., the dominant mechanism is DWM. To take its contribution into account we proceeded to sum $\kappa_{r\perp}$ calculated above and $\kappa_{d\perp}$ calculated using Eqs. (12) and (13) with two adjustable parameters, E_0 and W/κ_0. The total $\kappa_\perp$, which had thus become a complex number, was then corrected for demagnetization, finally yielding $\chi_\perp'$ and $\chi_\perp''$. A reasonable agreement with experiment for $\chi_\perp'$ was obtained with the values

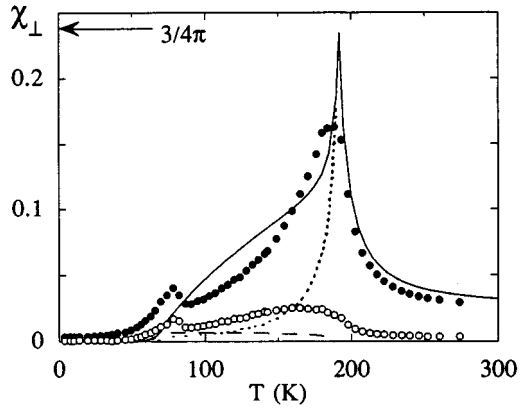

FIG. 5. Transverse external ac susceptibility: (●) real component, experiment; (○) imaginary component, experiment; (—) real component including the DWM contribution, calculation; (···) real component excluding the DWM contribution; (---) imaginary component, calculation.

$E_0=1.5\times10^3$ K and $W/\kappa_{0\perp}=1.5\times10^4$ K and is shown as the continuous line below T_2. With these parameters the DWM contribution sets on at $T\approx80$ K. The resulting curve is of the correct magnitude, although it is sharper than the experimental one. Besides, our model correctly predicts a nonzero imaginary component $\chi_\perp''$ for $T<T_2$. However, the amplitude of $\chi_\perp''$ is considerably lower than in the experiment.

The same procedure was applied to interpret $\chi_\parallel$. The $\kappa_{r\parallel}$ contribution shows a steplike increase from $\kappa_{r\parallel}=0$ above T_2 to a finite value below T_2, and a spike at T_1 (see Fig. 2, inset) resembling qualitatively the two cusps observed experimentally in $\chi_\parallel'$. However, this contribution is found to be two orders of magnitude lower than the experiment, so it is clear that the predominant contribution to the susceptibility in the parallel direction is that due to DWM. The DWM contribution was calculated with Eqs. (12) and (13) and corrected for demagnetization factor (full line Fig. 2). The adjustable parameters were $E_0=2\times10^3$ K and $W/\kappa_0=8\times10^3$ K. The difference in the values of W/κ_0 and E_0 for the parallel and perpendicular susceptibilities could be expected since those values are related to two different types of domain walls. The anomaly at T_1 is predicted as well as the continuous growth, essentially due to DWM, for $T>80$ K. Besides, a nonzero $\chi_\parallel''$ component also appears for $T>80$ K but is much lower than the experiment. Thus, the general features of the susceptibility components have been reproduced, as shown in Figs. 2 and 5: $\chi_\parallel'$ grows with temperature and $\chi_\perp'$ has a sharp peak at T_2.

In Fig. 6 we have depicted together with the frequency dependence of $\chi_\parallel'$ at $T=150$ K, i.e., below T_2, the theoretical prediction calculated with Eq. (12) and the parameters obtained in the temperature dependence fitting. We see that the frequency dependence also agrees reasonably well with experiment.

The main discrepancy is encountered at T_1, where our naive model predicts discontinuities corresponding to the first-order SRT. These discontinuities may be smoothed out by taking into account the previously established coexistence of two phases in a broad temperature interval around T_1,[9] however even then the broad maxima observed near $T=80$ K in $\chi_\perp'$ and $\chi_\perp''$ would not be reproduced.

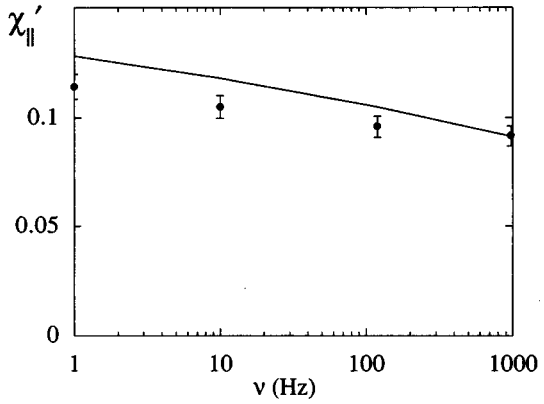

FIG. 6. Frequency dependence of $\chi_{\parallel}'$ at $T=150$ K: (●) experiment; (—) calculation.

Another region difficult to fit is the vicinity of the second transition point, T_2. It is not too surprising that the peak in $\chi_{\perp}'$ is rounded out and $\chi_{\perp}''$ has a high-temperature ''tail,'' as our model is not valid near T_2, where the domain width d and the wall thickness δ are of the same order of magnitude.

The dip observed in $\chi_{\parallel}'$ and $\chi_{\parallel}''$ near T_2 is not predicted by our model. Such a dip was also observed in $Nd_2Fe_{14}B$ under similar conditions[4] as well as in $TbFe_{11}Ti$.[28] It is likely to constitute a characteristic attendant feature of this type of spin reorientation transitions. It should be noted that the temperature dependence of the anisotropy constants does not provide a simple explanation of this effect. Indeed, the domain width, wall energy, and thickness are determined by $K_{\rm eff}$ rather than K_1 and therefore do not show any singularity at $T=T_2$.

IV. CONCLUSION

The ac susceptibility of a spherical single crystal of $DyFe_{11}Ti$ has been measured along the principal crystallographic directions at various temperatures and frequencies. A theoretical model has been proposed allowing for coherent magnetization rotation and domain-wall motion, which provides a satisfactory quantitative description of the real component of the observed susceptibility, χ', and a qualitative description of its imaginary component, χ''.

In particular, domain-wall motion is shown to be chiefly responsible for the growing with temperature real part of the susceptibility along the fourfold axis, $\chi_{\parallel}'$, as well as for the growth of $\chi_{\perp}'$ below the spin reorientation point T_2, whereas coherent rotation accounts for the ''tail'' of $\chi_{\perp}'$ above its peak at T_2. A dip in the temperature dependence has been clearly detected at $T=T_2$; it is believed to be a common feature of this class of spin reorientation transitions. Its nature, however, remains to be clarified.

ACKNOWLEDGMENTS

The authors wish to thank Professor J.M.D. Coey for providing the single crystal and for helpful discussions. This work was supported by CICYT Project MAT 93-0240-C04-04. It forms a part of the Concerted European Action on Magnets, an EU project. M.D.K. acknowledges financial support from SB 93-A0KIII150 of Ministerio de Educación y Ciencia of Spain. The microscopic photograph (Fig. 4) was made by Dr. A. Larrea.

APPENDIX A: ANISOTROPY CONSTANTS AND ORIENTATION OF THE EASY AXIS

The anisotropy constants entering Eq. (1) consist of two parts contributed by the iron and the rare-earth sublattices,

$$K_j=K_{j\rm Fe}+K_{jR}. \tag{A1}$$

the rare-earth contribution is calculated in the linear approximation,[29]

$$\begin{aligned}
K_{1R}&=-3J^2B_{20}B_J^2(x)-40J^4B_{40}B_J^4(x)-168J^6B_{60}B_J^6(x),\\
K_{2R}&=35J^4B_{40}B_J^4(x)+378J^6B_{60}B_J^6(x),\\
K_{3R}&=-231J^6B_{60}B_J^6(x),\\
K_{2R}'&=J^4B_{44}B_J^4(x)+10J^6B_{64}B_J^6(x),\\
K_{3R}'&=-11J^6B_{64}B_J^6(x),\\
x&=5\mu_B n_{R\rm Fe}M_{\rm Fe}(T)/kT,
\end{aligned} \tag{A2}$$

where $B_J^n(x)$ are the generalized Brillouin functions defined in Ref. 29; the CF and exchange parameters are taken from Ref. 6, $B_{20}=0.16$ K, $B_{40}=1.1\times10^{-3}$ K, $B_{44}=1.05\times10^{-2}$ K, $B_{60}=1.6\times10^{-5}$ K, $B_{64}=-4.0\times10^{-6}$ K, and $n_{R\rm Fe}=4\pi\times141$. The iron sublattice magnetization is approximated by the following empirical formula:[30]

$$M_{\rm Fe}(T)=M_{\rm Fe}(0)(1.9\sqrt{t}-0.9t),\quad t=1-T/T_C, \tag{A3}$$

with $M_{\rm Fe}(0)=1.0$ kG (Ref. 6) and $T_C=534$ K (Ref. 5) [Eqs. (A2) give the K_{jR} in K/fu and to be translated into erg/cm^3 they should be multiplied by 8.05×10^5].

The iron sublattice contribution to K_1 is interpolated as follows:[30]

$$K_{1\rm Fe}(T)=K_{1\rm Fe}(0)(0.81t+1.38t^2-1.19t^3), \tag{A4}$$

where $K_{1\rm Fe}(0)$ is taken equal to the K_1 of $YFe_{11}Ti$, 2.0×10^7 erg/cm^3, Ref. 31. Iron sublattice contributions to higher-order anisotropy constants are neglected.

The angle θ between the easy axis and the [001] direction is set to zero when $K_1>0$; if $K_1<0$, the value of θ is taken equal to either θ_0 or $\pi/2$, whichever delivers a smaller value to the anisotropy energy, Eq. (2), where

$$\sin^2\theta_0=\frac{\sqrt{\overline{K_2^2}-3K_1\overline{K_3}}-\overline{K_2}}{3\overline{K_3}}. \tag{A5}$$

APPENDIX B: SUSCEPTIBILITY DUE TO COHERENT ROTATION

Let the orientation of the spontaneous magnetization and applied magnetic field with respect to the crystallographic coordinate system be described by spherical angles (θ,φ) and (α,β), respectively. We shall consider the general case, $\theta\neq0$, the answer for the essentially different particular case $\theta=0$ being well known:[27]

$$\kappa_{r\parallel}=0, \tag{B1}$$

$$\kappa_{r\perp}=M_s^2/2K_1. \tag{B2}$$

When $\theta\neq 0$, the initial rotational susceptibility along the direction of the field is given by

$$\kappa_r=M_s\left\{[\cos\theta\,\sin\alpha\,\cos(\varphi-\beta)-\sin\theta\,\cos\alpha]\left(\frac{d\theta}{dH}\right)_{H=0}\right.$$
$$\left.-\sin\theta\,\sin\alpha\,\sin(\varphi-\beta)\left(\frac{d\varphi}{dH}\right)_{H=0}\right\}. \tag{B3}$$

To find the derivatives entering Eq. (B3), we minimize the free energy,

$$F=F_a-M_sH[\cos\theta\,\cos\alpha+\sin\theta\,\sin\,\alpha\cos(\varphi-\beta)], \tag{B4}$$

with respect to θ and φ; then the necessary conditions of minimum are derivated with respect to H, and H is set to zero. Thus we get

$$\left(\frac{d\theta}{dH}\right)_{H=0}=2D_1M_s[\cos\theta\,\sin\alpha\,\cos(\varphi-\beta)-\sin\theta\,\cos\alpha], \tag{B5}$$

$$\left(\frac{d\varphi}{dH}\right)_{H=0}=2D_2M_s\,\frac{\sin\alpha\,\sin(\beta-\varphi)}{\sin\theta}, \tag{B6}$$

where we have taken into account that if $H=0$ the equilibrium is reached at $\phi=\pi/4+n\pi/2$, where $\partial^2F_a/\partial\theta\partial\varphi=0$, $\partial^2F_a/\partial\theta^2=1/(2D_1)$, and $\partial^2F_a/\partial\varphi^2=(\sin^2\theta)/(2D_2)$,

$$D_1=[4K_1(1-2\sin^2\theta)+8\overline{K_2}(3\sin^2\theta-4\sin^4\theta)$$
$$+12\overline{K_3}(5\sin^4\theta-6\sin^6\theta)]^{-1}, \tag{B7}$$

$$D_2=[32\sin^2\theta(K_2'+K_3'\sin^2\theta)]^{-1}. \tag{B8}$$

Substituting Eqs. (B5) and (B6) into (B3), we arrive at the following general answer:

$$\kappa_r=2M_s^2\left\{D_1\left[\cos\theta\,\sin\alpha\,\cos\left(\frac{\pi}{4}+\frac{n\pi}{2}-\beta\right)-\sin\theta\,\cos\alpha\right]^2\right.$$
$$\left.+D_2\sin^2\alpha\,\sin^2\left(\frac{\pi}{4}+\frac{n\pi}{2}-\beta\right)\right\}. \tag{B9}$$

Finally, putting in Eq. (B9) $\alpha=0$ and $\pi/2$, we get

$$\kappa_{r\parallel}=2M_s^2D_1\sin^2\theta, \tag{B10}$$

$$\kappa_{r\perp}=2M_s^2\left[D_1\cos^2\theta\,\cos^2\left(\frac{\pi}{4}+\frac{n\pi}{2}-\beta\right)\right.$$
$$\left.+D_2\sin^2\left(\frac{\pi}{4}+\frac{n\pi}{2}-\beta\right)\right]. \tag{B11}$$

The transverse susceptibility, appears to depend essentially on the domain structure. Suppose that only the $n=2$ domains are present. Then, for the principal directions in the basal plane one has

$$\beta=0:\quad \kappa_{r[100]}=M_s^2(D_1\cos^2\theta+D_2), \tag{B12}$$

$$\beta=\pi/4:\quad \kappa_{r[110]}=2M_s^2D_1\cos^2\theta, \tag{B13}$$

$$\beta=\pi/2:\quad \kappa_{r[010]}=M_s^2(D_1\cos^2\theta+D_2), \tag{B14}$$

$$\beta=3\pi/4:\quad \kappa_{r[1\bar{1}0]}=2M_s^2D_2. \tag{B15}$$

In this case, if $D_2\ll D_1$, then $\kappa_{r[110]}\approx 2\kappa_{r[100]}$.

If now one assumes that the domains with $n=1$, 2, 3, and 4 are distributed equiprobably, then

$$\left\langle\sin^2\left(\frac{\pi}{4}+\frac{n\pi}{2}-\beta\right)\right\rangle=\left\langle\cos^2\left(\frac{\pi}{4}+\frac{n\pi}{2}-\beta\right)\right\rangle=\frac{1}{2} \tag{B16}$$

and

$$\kappa_{r[100]}=\kappa_{r[110]}=\kappa_{r\perp}=M_s^2(D_1\cos^2\theta+D_2). \tag{B17}$$

This settles the dispute between Refs. 4 and 11 on whether $\kappa_{r[110]}$ should be twice as large as $\kappa_{r[100]}$ or equal to it. The authors of the two works simply proceeded from different assumptions. Our data (Fig. 1) indicate that $\chi_{[110]}=\chi_{[100]}$ everywhere except the neighborhood of the point T_2, where both susceptibilities are determined mainly by the shape of the sample. As the latter was only approximately spherical, the difference between $\chi_{[110]}$ and $\chi_{[100]}$ observed near T_2 should be attributed to the sample's asphericity, rather than to anisotropy of κ in the basal plane. Thus, equiprobable distribution of domains is adopted in the present work.

[1] J. Bartolomé, L. M. García, F. J. Lázaro, Y. Grincourt, L. G. de la Fuente, C. de Francisco, J. M. Muñoz, and D. Fruchart, IEEE Trans. Magn. **30**, 577 (1994).

[2] L. M. García, J. Bartolomé, F. J. Lázaro, C. de Francisco, J. M. Muñoz, and D. Fruchart, J. Magn. Magn. Mater. **140–144**, 1049 (1995).

[3] L. M. García, Ph.D thesis, Universidad de Zaragoza, 1994.

[4] D.-X. Chen, V. Skumryev, and H. Kronmüller, Phys. Rev. B **46**, 3496 (1992).

[5] P.-B. Hu, H.-S. Li, J. P. Gavigan, and J. M. D. Coey, J. Phys. Condens. Matter **1**, 755 (1989).

[6] B.-P. Hu, H.-S. Li, J. M. D. Coey, and J. P. Gavigan, Phys. Rev. B **41**, 2221 (1990).

[7] A. V. Andreev, M. I. Bartashevich, N. V. Kudrevatykh, S. M. Razgonyaev, S. S. Sigaev, and E. N. Tarasov, Physica B **167**, 139 (1990).

[8] L. M. García, J. Bartolomé, P. A. Algarabel, M. R. Ibarra, and M. D. Kuz'min, J. Appl. Phys. **73**, 5908 (1993).

[9] P. A. Algarabel, M. R. Ibarra, J. Bartolomé, L. M. García, and M. D. Kuz'min, J. Phys. Condens. Matter **6**, 10 551 (1994).

[10] J. Bartolomé, in *Interstitial Intermetallic Alloys*, Vol. E-281 of NATO Advanced Study Institute, Series E: Physics, edited by G.

J. Long, F. Grandjean, and K. H. J. Buschow (Kluwer, Dordrecht, 1995), Chap. 24, p. 601.

[11] C. Rillo, F. Lera, A. Badía, L. A. Angurel, J. Bartolomé, F. Palacio, R. Navarro, and A. J. van Duyneveldt, in *Magnetic Susceptibility of Superconductors and Other Spin Systems*, edited by R. A. Hein (Plenum, New York, 1991), p. 1.

[12] C. Rillo, J. Chaboy, R. Navarro, J. Bartolomé, D. Fruchart, B. Chenevier, A. Yaouanc, M. Sagawa, and S. Hirosawa, J. Appl. Phys. **64**, 5534 (1988).

[13] R. B. Goldfarb, M. Lelental, and C. A. Thompson, in *Magnetic Susceptibility of Superconductors and Other Spin Systems* (Ref. 11), p. 49.

[14] D.-X. Chen, *Physical Basis of Magnetic Measurements* (China Mechanical Industry, Beijing, 1985), pp. 139–140.

[15] A. Larrea (private communication).

[16] R. Szymczac, J. Zawadzki, D. H. Mahn, and M. Slepowronski, J. Magn. Magn. Mater. **104–107**, 321 (1992).

[17] R. Szymczac, J. Zawadzki, Z. Drzazga, and R. Szymczac, J. Magn. Magn. Mater. **83**, 267 (1990).

[18] W. D. Corner and M. J. Hawton, J. Magn. Magn. Mater. **72**, 59 (1988).

[19] W. Wójcik, E. Jędryka, P. Panissod, and K. H. J. Buschow, J. Magn. Magn. Mater. **83**, 243 (1990).

[20] J. J. van den Broek and H. Zijlstra, IEEE Trans. Magn. **7**, 226 (1971).

[21] H.-R. Hilzinger and H. Kronmüller, Phys. Status Solidi B **54**, 593 (1972); **59**, 71 (1973).

[22] H. M. Mayer, M. Steiner, N. Stüβer, H. Weinfurter, K. Kakurai, B. Dorner, P. A. Lindgård, K. N. Clausen, S. Hock, and W. Rodewald, J. Magn. Magn. Mater. **97**, 210 (1991).

[23] C. Herring and C. Kittel, Phys. Rev. **81**, 869 (1951).

[24] K. H. J. Buschow, in *Ferromagnetic Materials*, Vol. 4, edited by E. P. Wolfarth and K. H. J. Buschow (North-Holland, Amsterdam, 1988), Chap. 1.

[25] C. Kittel and J. K. Galt, in *Solid State Physics: Advances in Research and Applications*, edited by F. Seitz and D. Turnbull (Academic, New York, 1956), Vol. 3.

[26] P. Gaunt, Philos. Mag. B **48**, 261 (1983).

[27] M. Kersten, Z. Angew. Phys. **8**, 313 (1956).

[28] A. V. Andreev, N. V. Kudrevatykh, S. M. Razgonyaev, and E. N. Tasarov, Physica B **183**, 379 (1993).

[29] M. D. Kuz'min, Phys. Rev. B **46**, 8219 (1992).

[30] M. D. Kuz'min and J. M. D. Coey, Phys. Rev. B **50**, 12 533 (1994).

[31] Q. Qi, Y. P. Li, and J. M. D. Coey, J. Phys. Condens. Matter **4**, 8209 (1992).